## SUPPLEMENTARY FIGURES

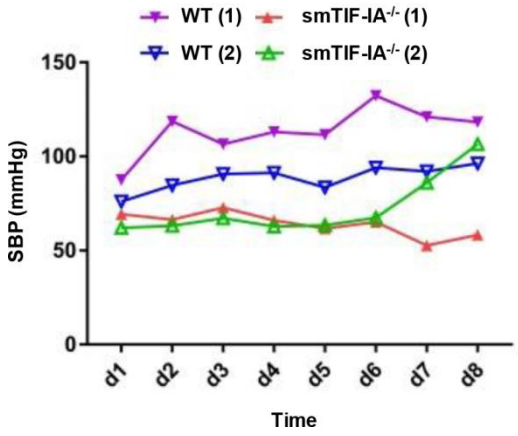


**Supplementary Figure 1. Comparison of conscious systolic blood pressures (SBP) in two smTIF-IA$^{-/-}$ mice versus two wild type littermates (WT), which were monitored for an 8-day period using a tail-cuff method (BP-2010A System, Softron Biotechnology, Beijing, China).**

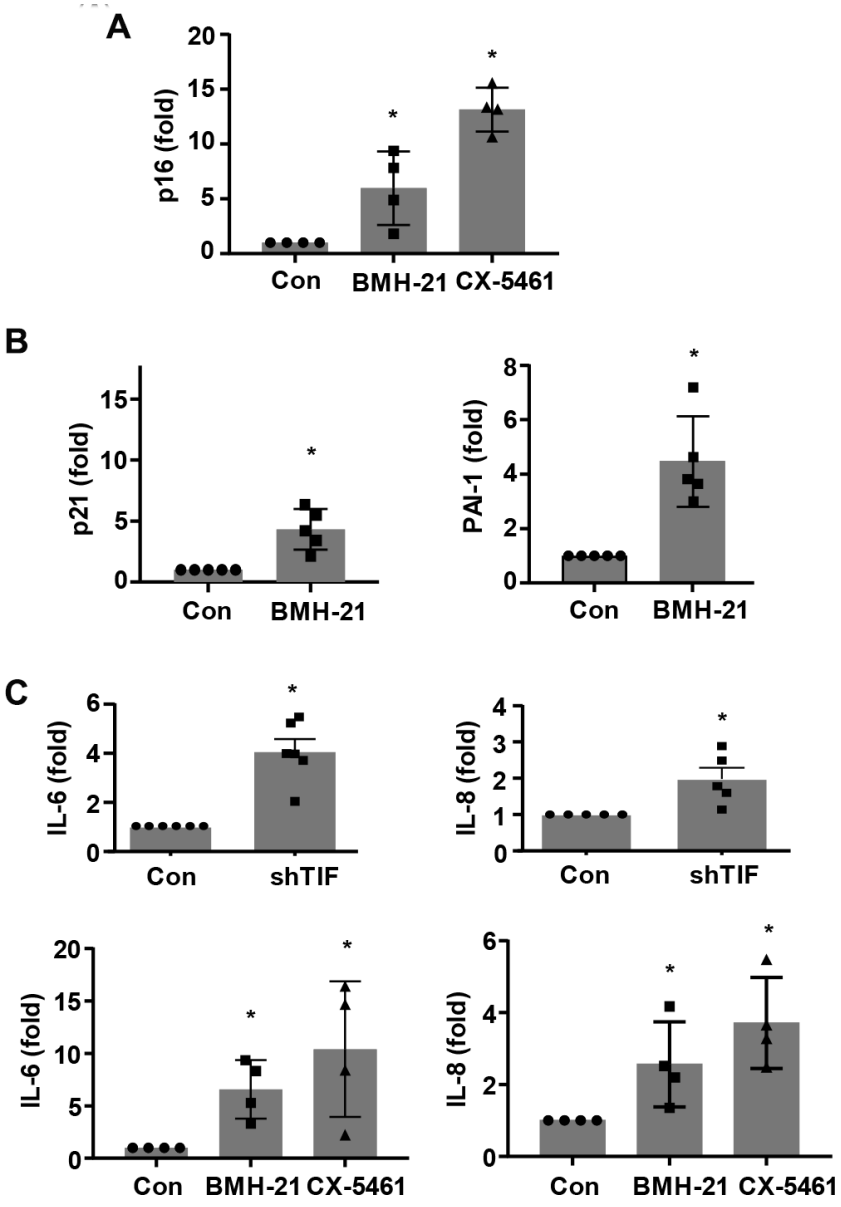


**Supplementary Figure 2. Effects of rDNA transcription inhibition on levels of various senescence markers in MOVAS cells detected by real-time PCR.** (**A**) Effects of CX-5461 (0.5 μM) and BMH-21 (0.5 μM) on the expression level of $p16^{INK4a}$. (**B**) Effects of BMH-21 (0.5 μM) on the expression levels of $p21^{Cip1}$ and PAI-1. (**C**) Effects of TIF-IA shRNA (shTIF), CX-5461 and BMH-21 on the expression levels of IL-6 and IL-8. * $P < 0.05$ versus control (Con), unpaired *t*-test or one-way ANOVA. The *n* number in each group was represented by the dots.

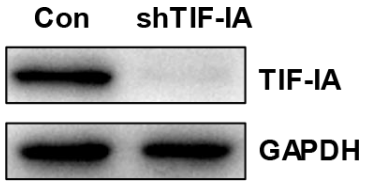


**Supplementary Figure 3. Example of western blots showing the effect of lentivirus-mediated TIF-IA shRNA transduction on the protein expression of TIF-IA in MOVAS cells.** A non-targeting sequence was used as control (Con).

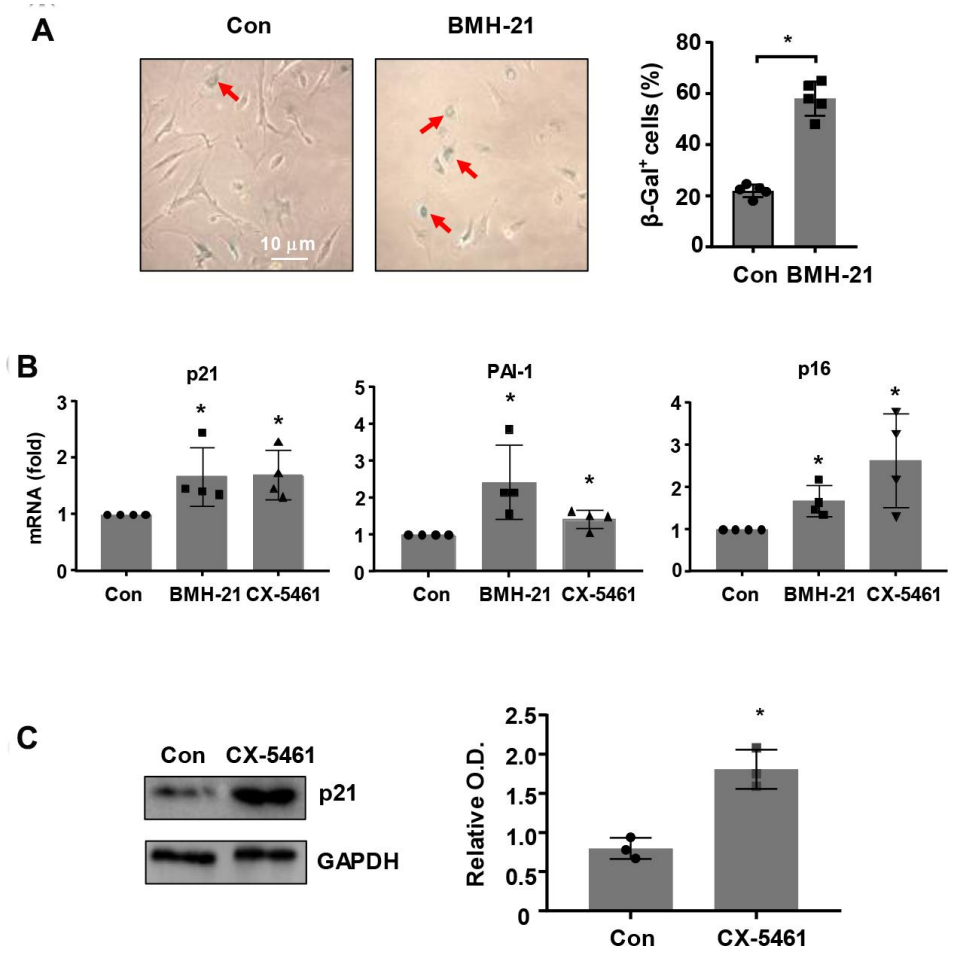


**Supplementary Figure 4. Effects of rDNA transcription inhibition on various senescence markers in human aortic smooth muscle cells (HASMCs).** (**A**) Effects of BMH-21 (5 μM) on the number of β-Gal-positive cells (blue color, arrows) after 5 days in culture. (**B**) Real-time PCR results showing CX-5461 (0.5 μM) and BMH-21 (5 μM) effects on the expression levels of $p21^{Cip1}$, PAI-1 and $p16^{INK4a}$. (**C**) Representative western blot and mean densitometry data showing the effect of CX-5461 on the protein level of $p21^{Cip1}$. * $P < 0.05$ versus control (Con), unpaired *t*-test or one-way ANOVA. Data were mean ± SD. The *n* number in each group was represented by the dots.

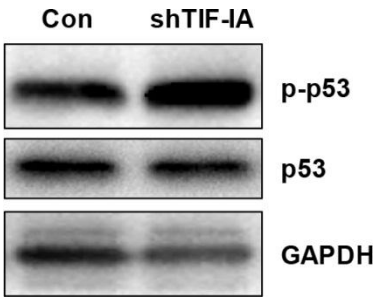


**Supplementary Figure 5. Representative western blot images showing increased p53 phosphorylation in TIF-IA gene-silenced MOVAS cells.** A non-targeting shRNA sequence was used as control (Con).

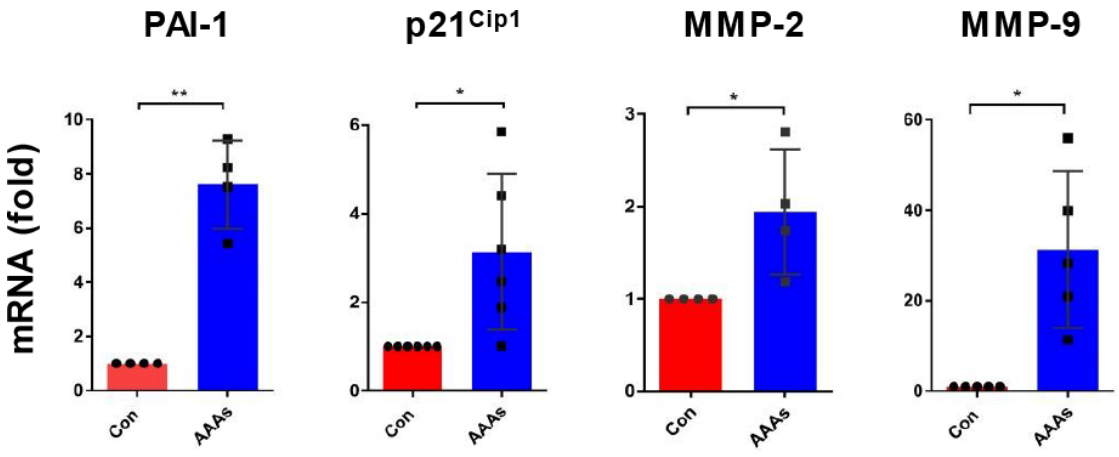


**Supplementary Figure 6. Real-time PCR results showing changes in the expression of PAI-1, p21$^{Cip1}$, MMP-2 and MMP-9 in human AAA tissues.** Data are expressed as dot blot-combined bar graphs representing mean ± SD. * $P < 0.05$, ** $P < 0.01$, unpaired *t*-test.

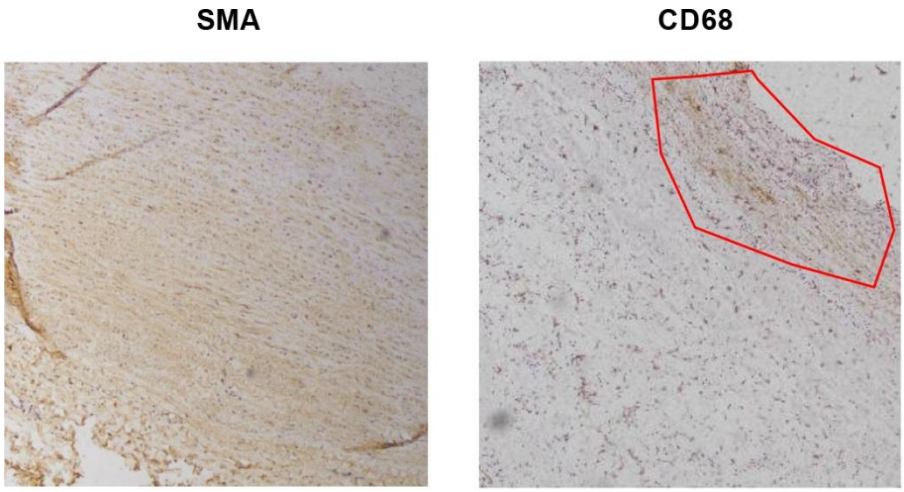


**Supplementary Figure 7. Immunohistochemistry images showing different distribution patterns of smooth muscle cells (SMA staining) and macrophages (CD68 staining) in human AAA tissues.** Sections were counterstained with hematoxylin. The red line indicated a macrophage-rich area. SMA, smooth muscle α-actin. Low power (40X) fields.

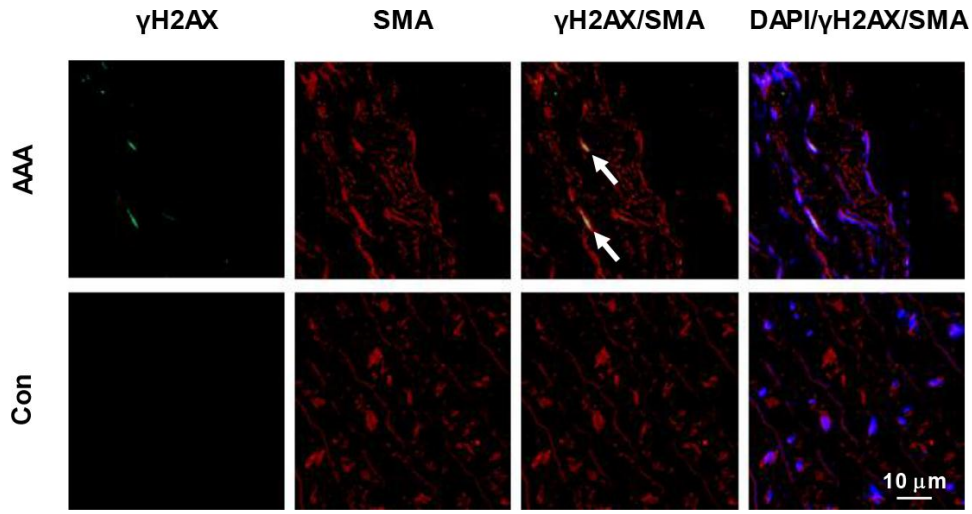


**Supplementary Figure 8. Double immunofluorescence labeling images showing that in human AAA sections, the majority of γH2AX signals co-localized with smooth muscle α-actin (SMA).** Nuclei were counterstained with DAPI.

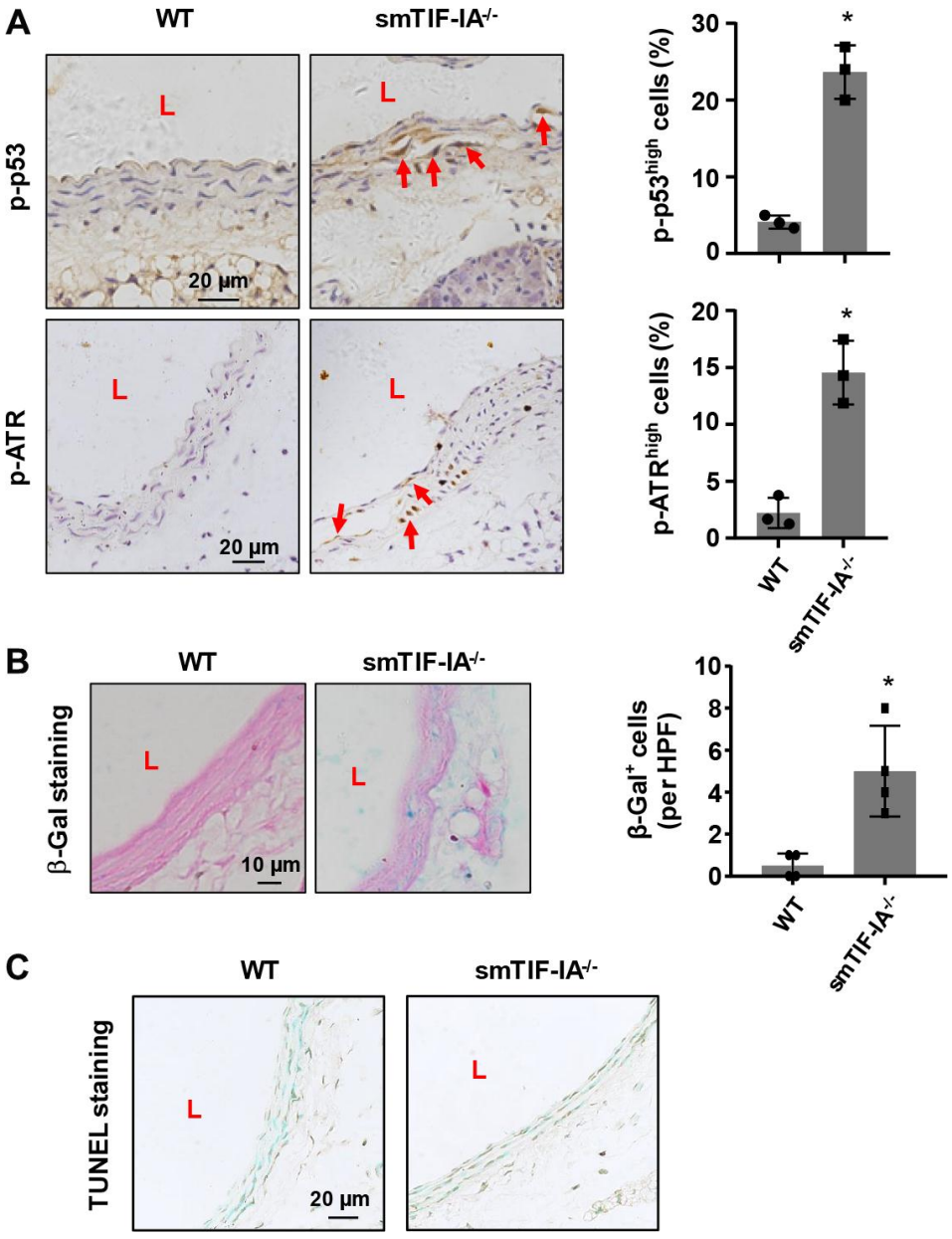


**Supplementary Figure 9. Changes in markers of senescence and apoptosis in the tunica media of smTIF-IA$^{-/-}$ aorta.** (**A**) Immunohistochemistry data showing the levels of phospho-p53 and phospho-ATR (arrows). Sections were counterstained with hematoxylin. (**B**) Representative images of β-Gal staining and quantitative data showing the presence of senescent cells (blue color) in the tunica media of smTIF-IA$^{-/-}$ aorta. (**C**) Terminal deoxynucleotidyl transferase dUTP Nick-End Labeling (TUNEL) staining showing that smTIF-IA$^{-/-}$ did not induce obvious cell apoptosis in the aorta, comparing with the wild type (WT) control. Data were mean ± SD. * $P < 0.05$ versus WT, unpaired *t*-test. L, lumen side of the vessel. HPF, high power field (100X oil immersion lens).

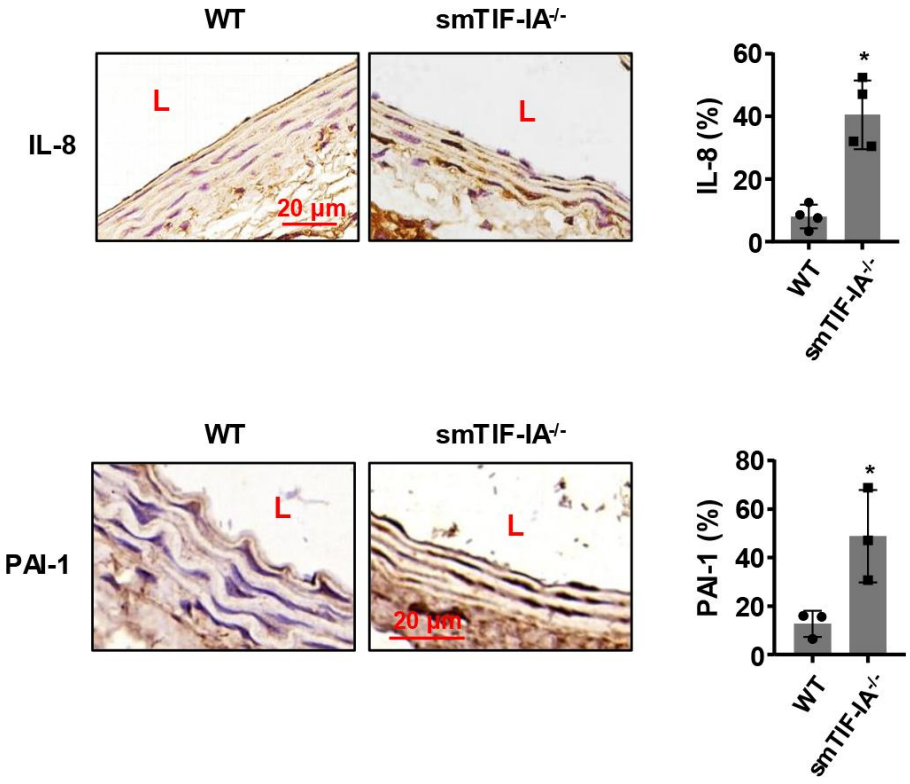


**Supplementary Figure 10. Changes in expression of SASP markers IL-8 and PAI-1 in smTIF-IA$^{-/-}$ aorta detected by immunohistochemistry.** Sections were counterstained with hematoxylin. Semi-quantitative data of immunoreactivity (% area) are shown on the right. Data were mean ± SD. * $P < 0.05$ versus wild type (WT), unpaired *t*-test. The *n* number in each group was represented by the dots. L, lumen side.